Microspacing In-Air Sublimation Growth of Organic Crystals

Xin Ye, Yang Liu*, Quanxiang Han, Chao Ge, Shuangyue Cui, Leilei Zhang, Xiaoxin Zheng, Guangfeng Liu, Jie Liu, Duo Liu and Xutang Tao*

State Key Laboratory of Crystal Materials, Shandong University, Jinan, Shandong 250100, P.R. China

Table of Contents

1. Thermal analyses of rubrene 2
2. TG/DSC and DSC analyses for rubrene in air 2
3. Real time observation of the sublimation process 3
4. MALDI-TOF spectra of rubrene 4
5. ^{13}C NMR spectra of rubrene starting materials and crystals grown by microspacing in-air sublimation. 4
6. ^{1}H NMR spectra of rubrene starting materials and crystals grown by microspacing in-air 5
7. Elemental analysis data for starting material and crystal grown by microspacing in-air sublimation of rubrene 5
8. Rotation and movement of crystal in the droplet 5
9. Real time process of using a much smaller amount of the starting material 6
10. Images of polycrystalline film and dendritic crystals grown on top substrate 6
11. Temperature dependence of the top substrate on different spacing distance 7
12. Controlled experiments of temperature difference 7
13. Comparison between the morphology of the grown crystals and the predicted crystal morphology 8
14. TG-DSC analyses 9
15. DSC analyses 10
16. Crystallization from melting intermediate 11
17. IR spectrum 12
18. Thermal analyses for pentacene, 1DPAFO, anthracene and TCNQ in air 13
19. Comparison of PVT and Microspacing In-Air Sublimation for growth of organic crystals on substrate 14
20. Experiment Section 15

1. Thermal analyses of rubrene

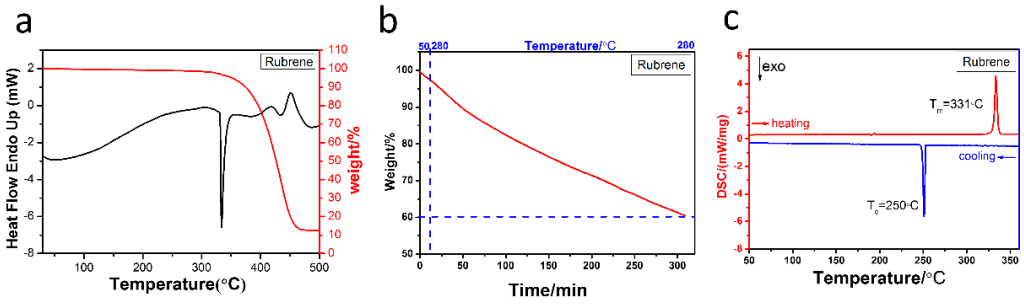

Figure S 1 Thermal analysis of rubrene. (a) Differential scanning calorimetry (DSC) and thermal gravimetric analysis (TGA) curves of rubrene powders at a rate of 10 °C min^{-1}. The red line is the TG curve and the black one is DSC curve. (b) TG curve of rubrene at 280 °C for 300min. (c) DSC analysis of rubrene at a rate of 10 °C min^{-1}. The black curve is the heating curve and the red one is the cooling curve. The Tc and Tm denote the recrystallization and melting temperatures respectively.

2. TG/DSC and DSC analyses for rubrene in air

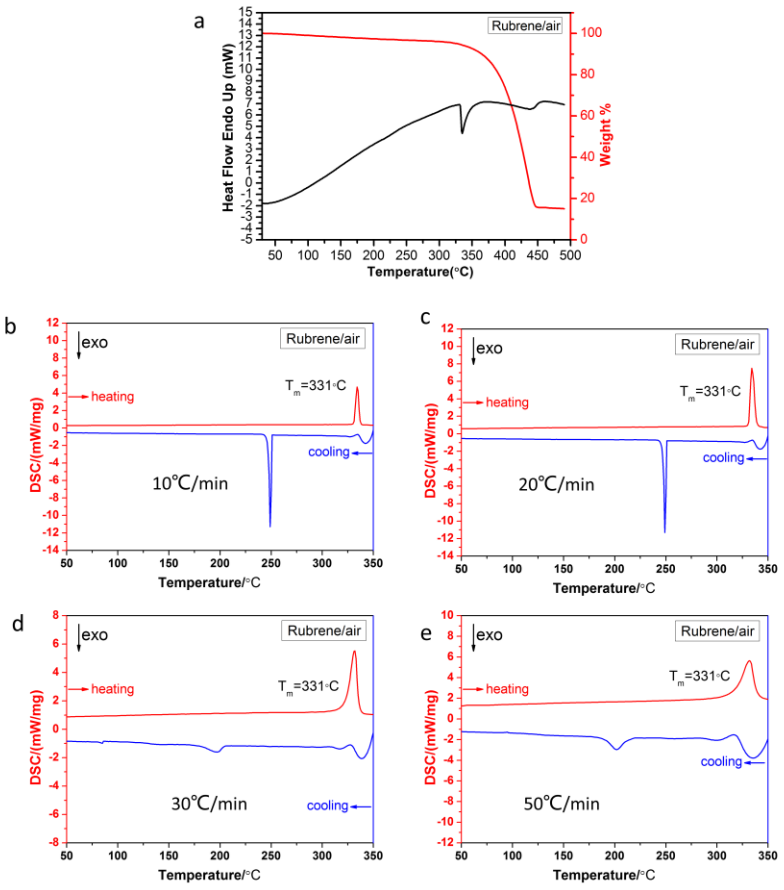

Figure S 2 TG/DSC (a) and DSC (b-e) analyses for rubrene in air at a rate of 10 °C min^{-1} (a and b), 20 °C min^{-1} (c), 30 °C min^{-1} (d) and 50 °C min^{-1} (e).

3. Real time observation of the sublimation process

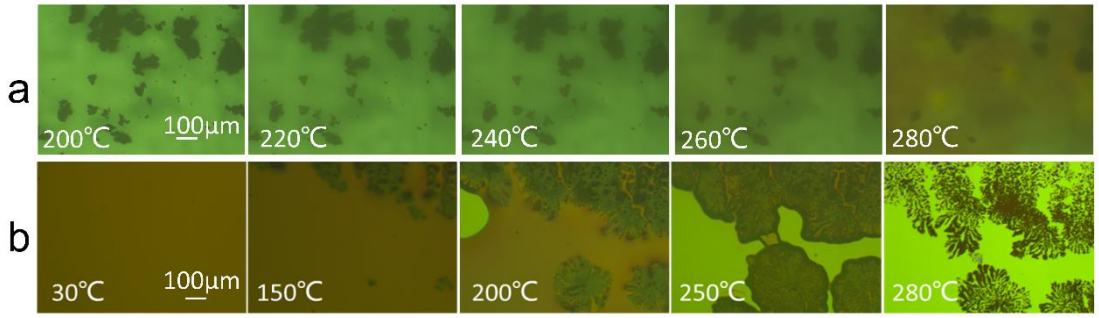

Figure S 3 Real time observation of the sublimation process on the bottom substrate during a temperature raising procedure. Hot-stage optical images of rubrene powder (a) at 200, 220, 240, 260, 280 °C and thin film (600μm, b) at 30, 150, 200, 250, 280 °C.

When we focused on the bottom substrate, during a temperature raising procedure (20 °C/min), the observed optical micrographs turned shady gradually after 220 °C, due to the volatilization of rubrene molecules from the bottom substrate and deposition on the top cover glass. After 260 °C, the transparency of the scene dropped severely and partial of the powders disappeared (Fig. S2a). To survey the sublimation more precisely, we fabricated thin film of rubrene on the bottom substrate via vacuum deposition. Following a same temperature raising procedure, we could see clearly the detachment of rubrene from the substrate. After 280 °C, most portion of the rubrene film disappeared and the surface of the substrate exposed (Fig. S2b). Besides the raise of the temperature, the relative sublimation rate was found to expedite likewise as the granularity decreasing and exposure surface enlarging of the sample. The film sample sublimated faster than the rubrene powders. This phenomenon, plus the constant temperature thermogravimetric analysis manifested that the sublimation of small-molecule compounds is a considerable thermal effect, even under atmospheric environment and a temperature much lower than the melting point. Although the mass loss in the meantime measured by the changing temperature thermogravimetry is negligible，the relative sublimed volume becomes significant when the total amount of the material is trace, and the exposure surface is large.

4. MALDI-TOF spectra of rubrene

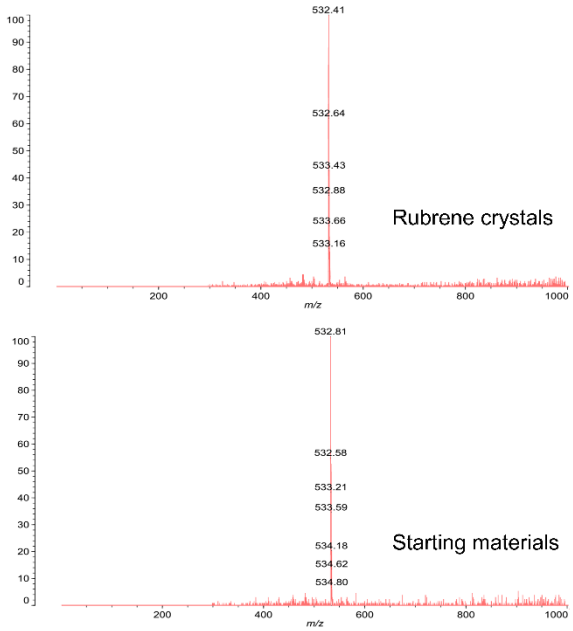

Figure S 4 MALDI-TOF spectra of the starting materials and grown crystals (obtained by scraping the materials from the upper substrate, containing solidified melt) of rubrene.

5. ^{13}C NMR spectra of rubrene starting materials and crystals grown by microspacing in-air sublimation.

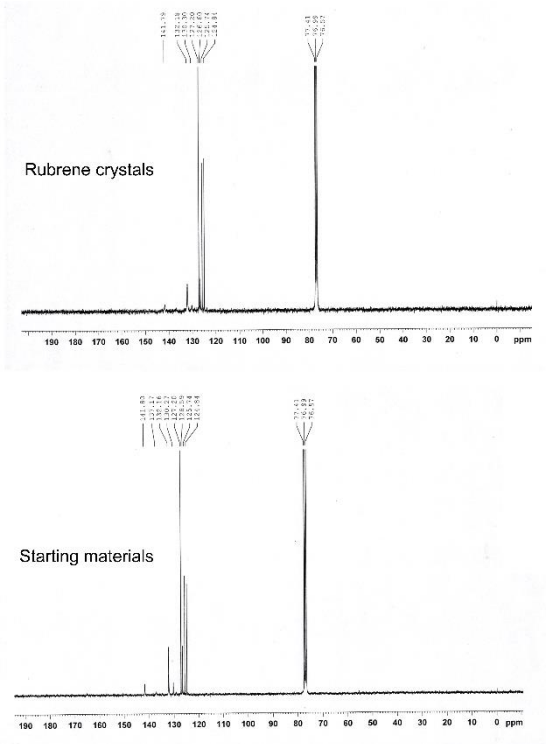

Figure S 5 ^{13}C NMR spectra of the starting materials and grown crystals (obtained by scraping the materials from the upper substrate, containing solidified melt) of rubrene.

6. ^{1}H NMR spectra of rubrene starting materials and crystals grown by microspacing in-air

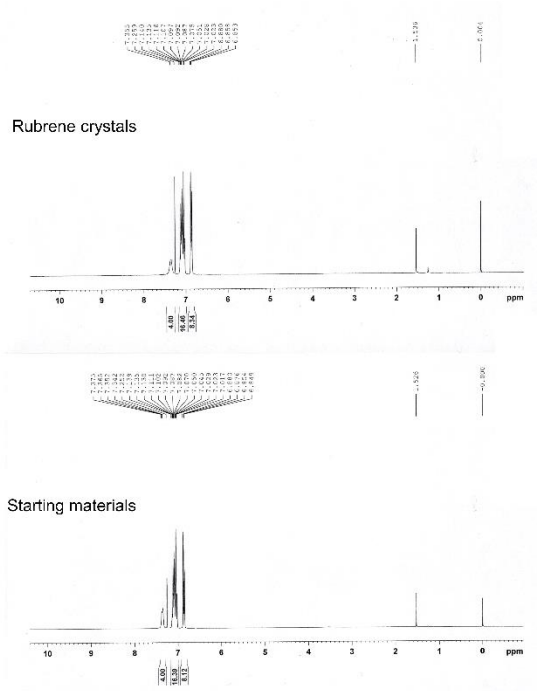

Figure S 6 ^{1}H NMR spectra of the starting materials and grown crystals (obtained by scraping the materials from the upper substrate, containing solidified melt) of rubrene.

7. Elemental analysis data for starting material and crystal grown by microspacing in-air sublimation of rubrene

Table S1. Elemental Analysis Data for Starting Material and Crystal Grown by Microspacing In-air Sublimation of Rubrene and Pentacene

element	TCI rubrene	rubrene crystals	TCI pentacene	pentacene crystals
%C	95.17(94.73)[a]	95.25	94.01(94.96)	94.01
%H	5.25(5.26)	5.27	4.81(5.04)	5.16

[a] Theoretical values in parentheses.

8. Rotation and movement of crystal in the droplet

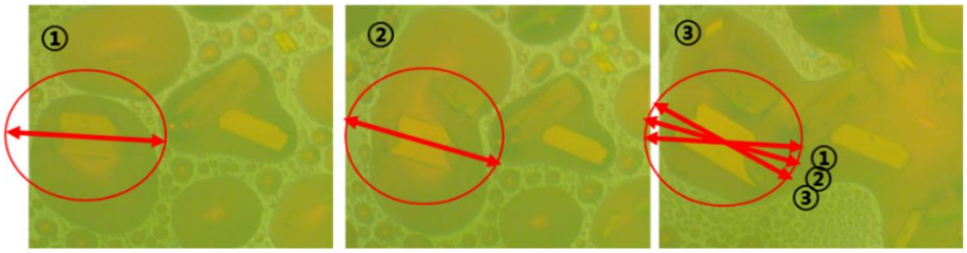

Figure S 7 Microscope images of rotation and movement of crystal in the droplet.

9. Real time process of using a much smaller amount of the starting material

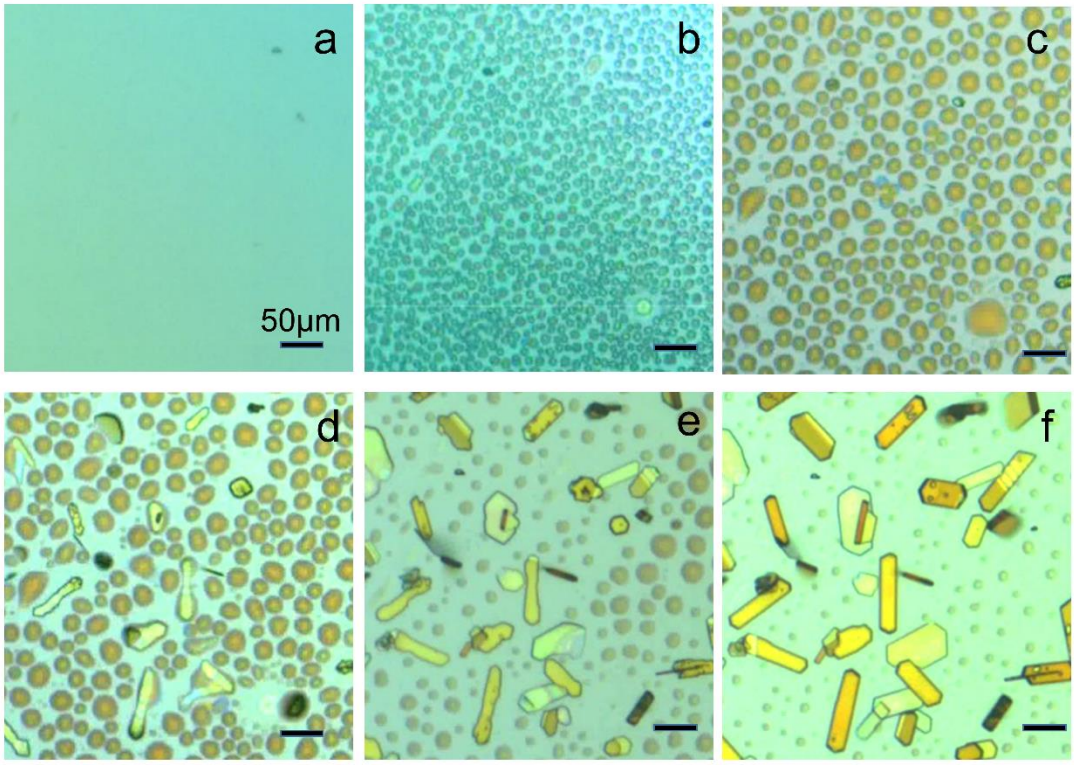

Figure S 8 Real time process of using a much smaller amount of the starting material (about one hundredth to that of Fig.3) via hot-stage microscope. Microscopy images focusing on the down surface of the quartz top substrate (a) before and (b)–(e) after heating to 280°C for b) 1 min, c) 3 min, (d) 5 min (e) 8 min and (f) 10 min.

10. Images of polycrystalline film and dendritic crystals grown on top substrate

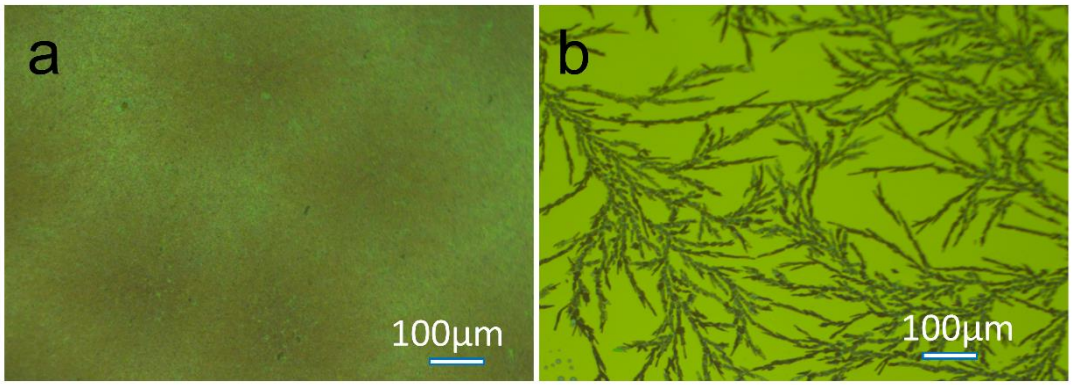

Figure S 9 Microscope images of polycrystalline film (a) and dendritic crystals (b) grown on top substrate (Si/SiO_2) of different sublimation distance. The distance is bigger than 4 mm for (a) and about 2mm for (b).

11. Temperature dependence of the top substrate on different spacing distance

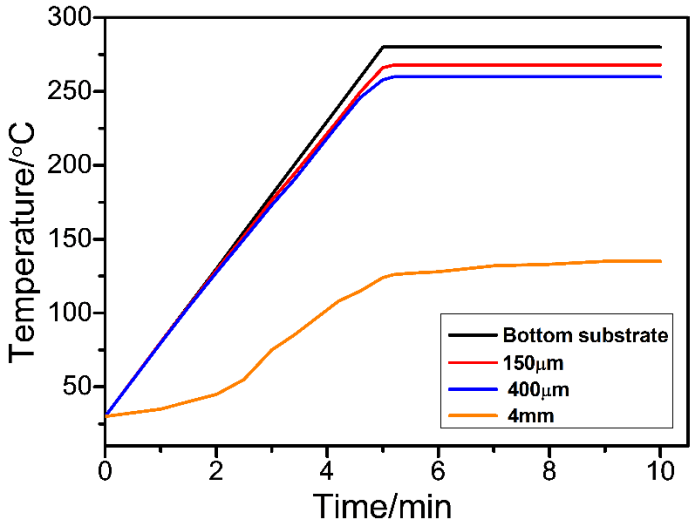

Figure S 10 Temperature curve of top substrate of different spacing distance.

12. Controlled experiments of temperature difference

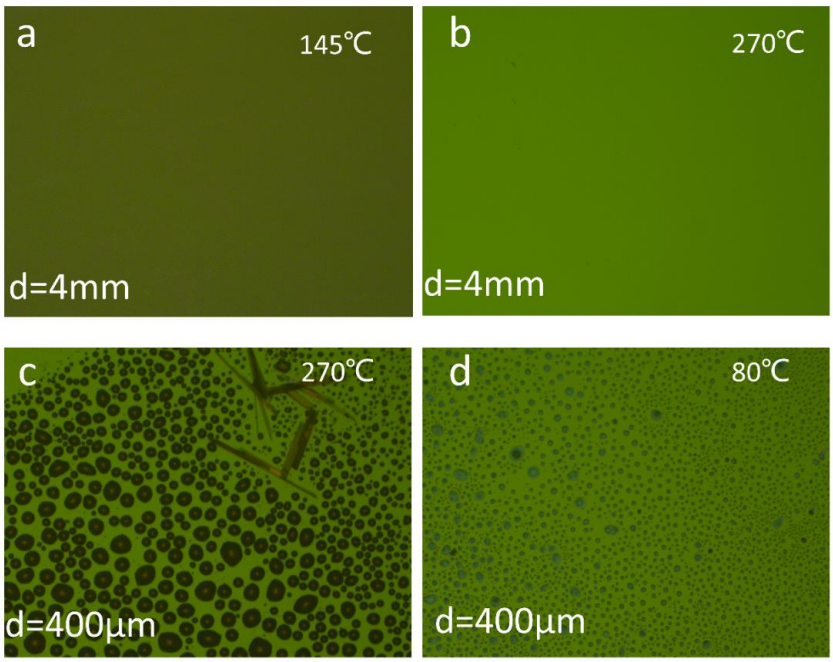

Figure. S 11 Controlled experiments by reducing the temperature difference between the two substrates in a larger spacing distance (b), or increasing the temperature difference in a microspacing distance (d). Microscope images of top substrate of different spacing distance (a and b is 4 mm, c and d is 400 μm) at different growth temperature (a is 145°C, b and c is 270°C, d is 80°C).

13. Comparison between the morphology of the grown crystals and the predicted crystal morphology

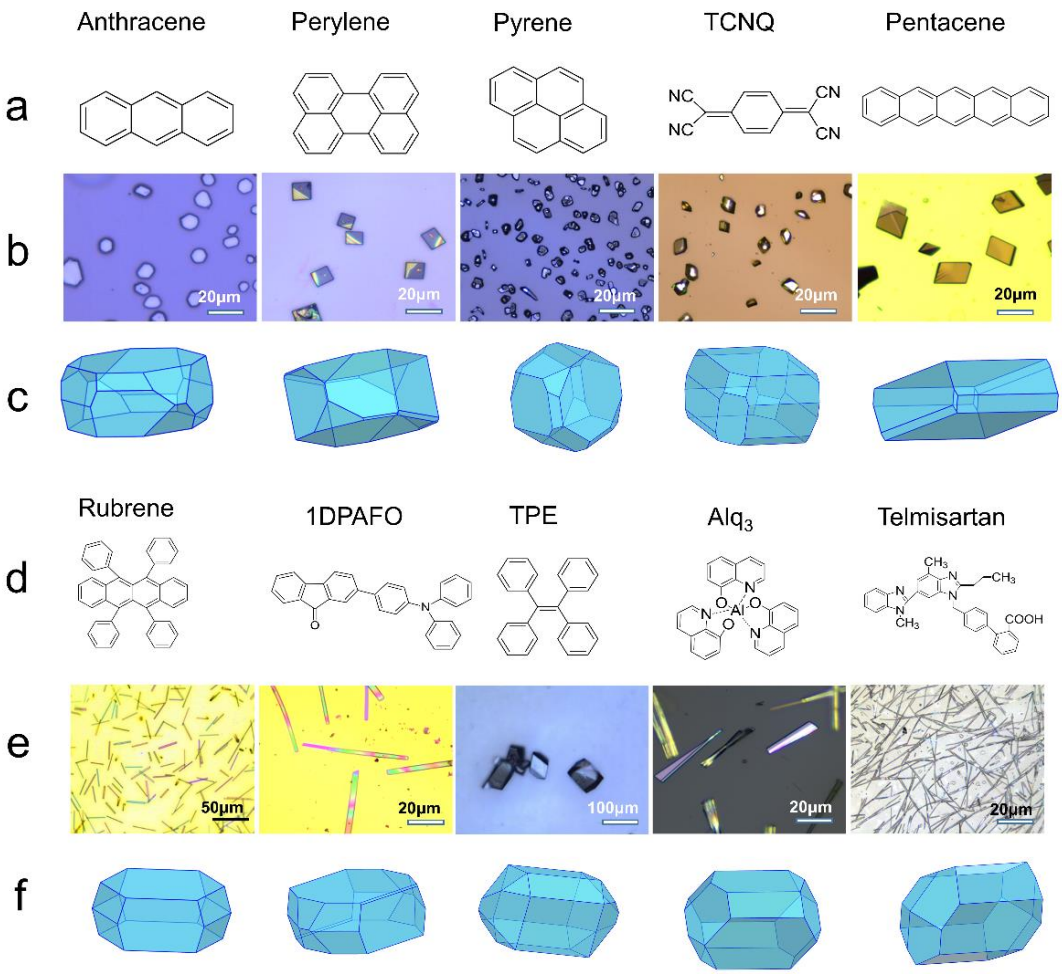

Figure S 12 (a and d) Chemical structures of the tested compounds anthrance, perylene, pyrene, TCNQ, pentacene, 1DOAFO, TPE, Alq_3, and telmisartan. (b and e) Microscope images. (c and f) The predicted crystal morphology based on the BFDH method.

14. TG-DSC analyses

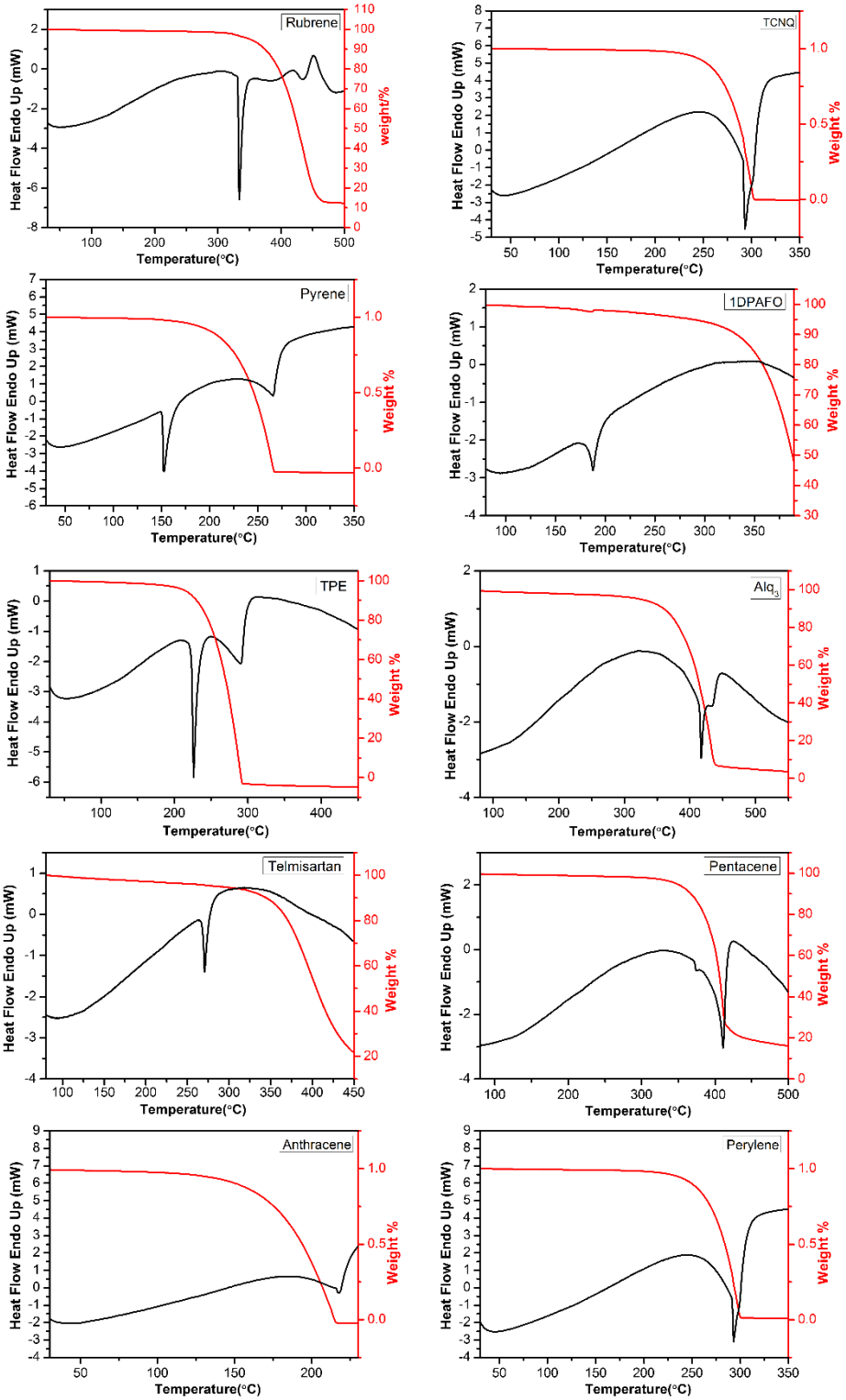

Figure S 13 TG/DSC analyses of rubrene, TCNQ, pyrene, 1DPAFO, TPE, Alq_3, pentacene, telmisartan, anthrance and perylene at a rate of 10°C min^{-1}. The red line is the TG curve and the black is the DSC curve.

15. DSC analyses

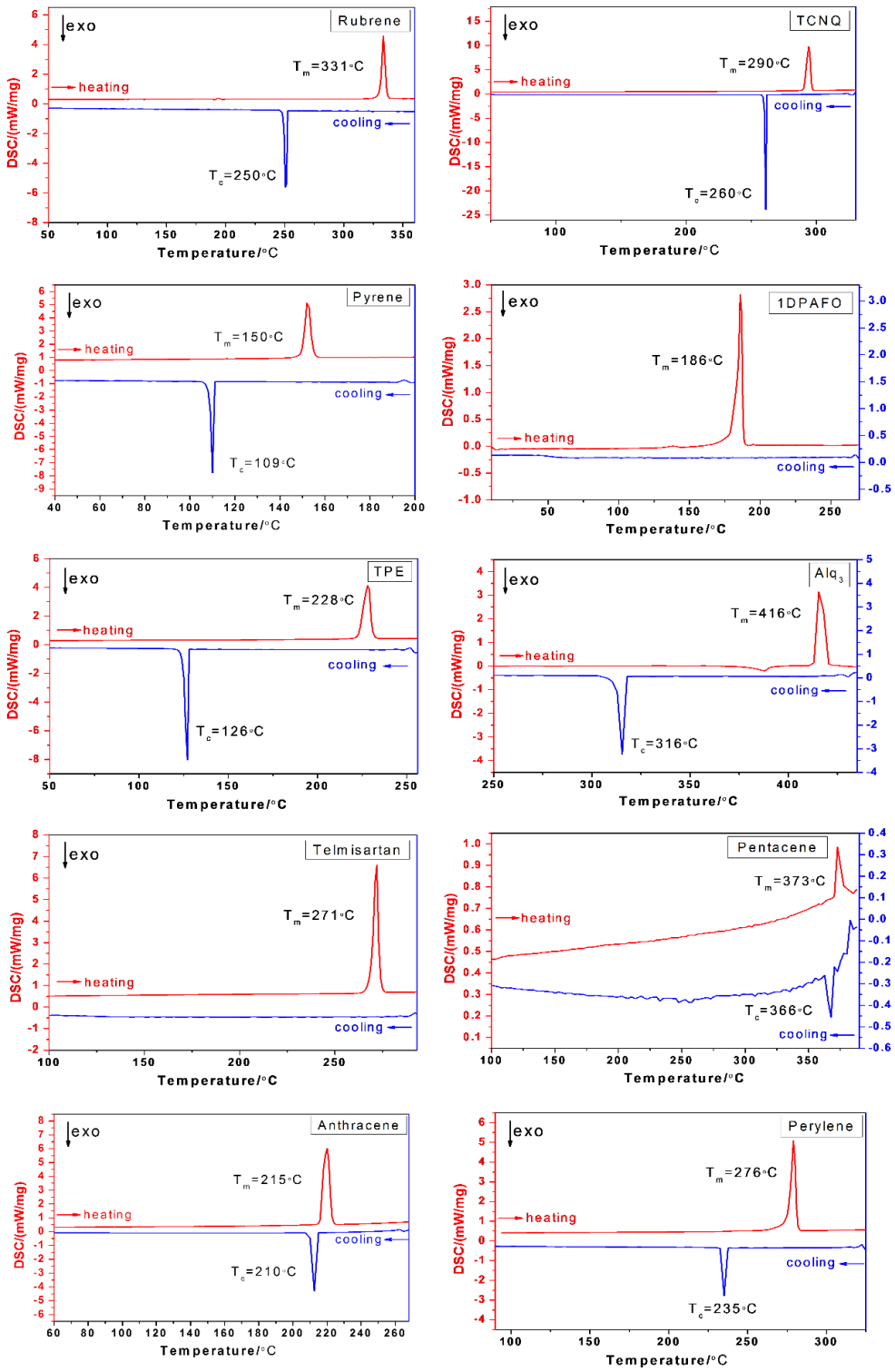

Figure S 14 DSC analyses of rubrene, TCNQ, pyrene, 1DPAFO, TPE, Alq_3, pentacene, telmisartan, anthrance and perylene at a rate of 10°C min_{-1}. The red curve is the heating curve and the blue one is the cooling curve. The Tc and Tm denote the recrystallization and melting temperatures respectively.

16. Crystallization from melting intermediate

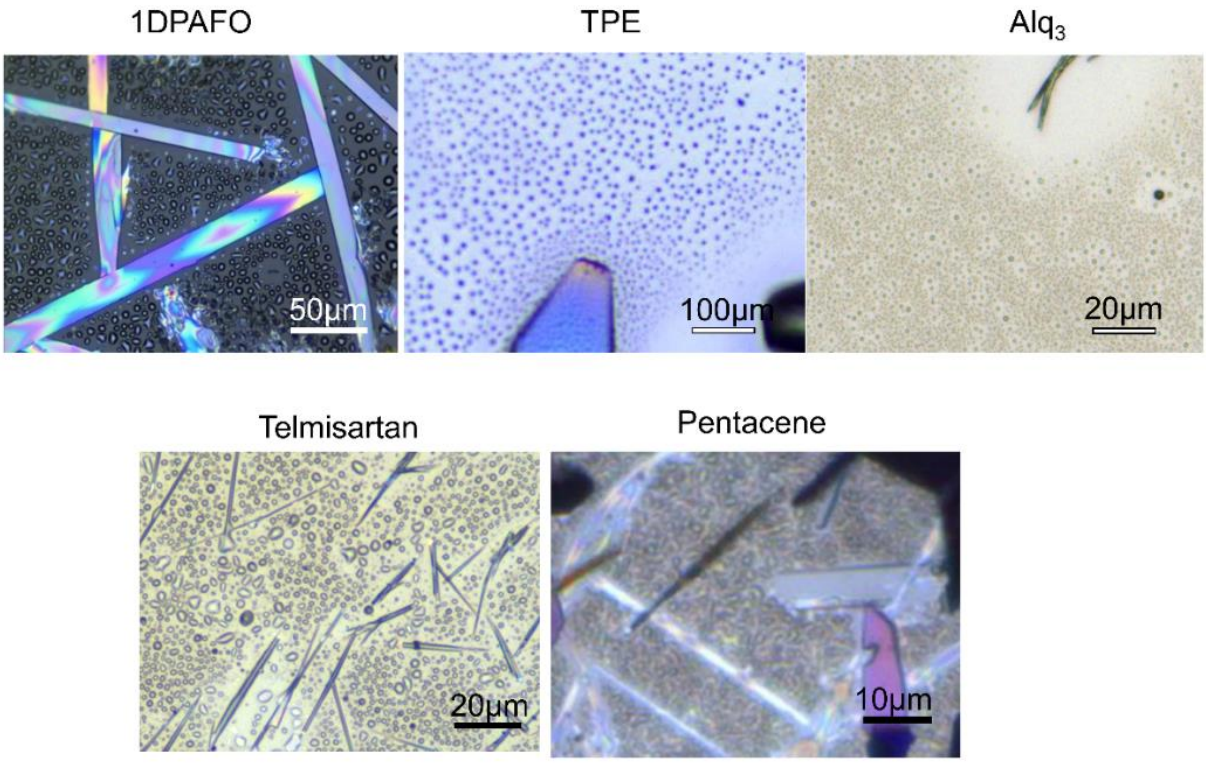

Figure S 15 Crystallization from melting intermediate was also observed for 1DPAFO, TPE, Alq_3, telmisartan, pentacene.

17. IR spectrum

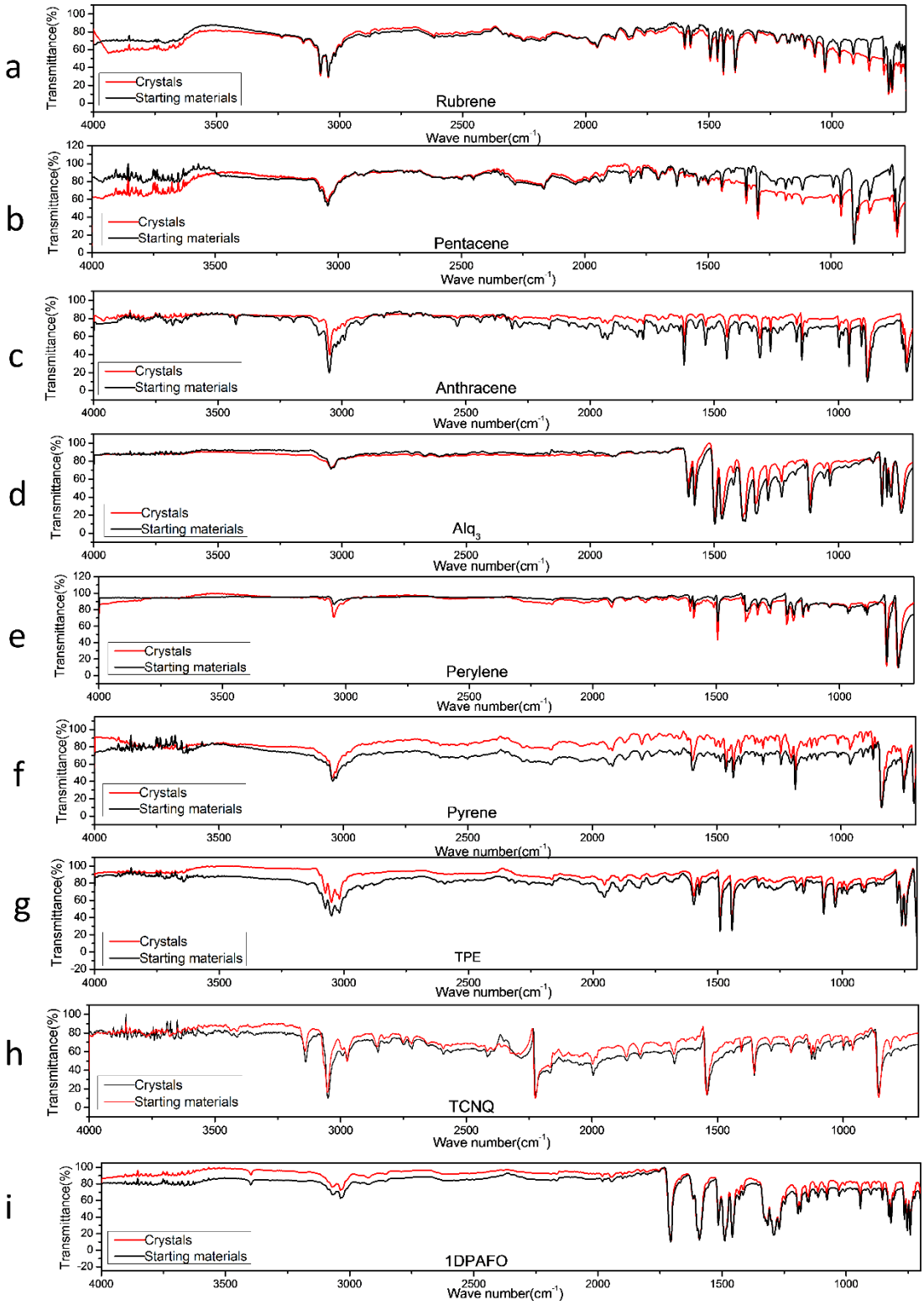

Figure S16 IR spectrum of starting materials and crystals (including some solidified droplet melt) grown by microspacing in-air sublimation of rubrene, pentacene, anthrance, Alq_3, perylene, pyrene, TPE, TCNQ, 1DPAFO. The red curve is for the crystal and the blue one is for the starting material.

18. Thermal analyses for pentacene, 1DPAFO, anthracene and TCNQ in air

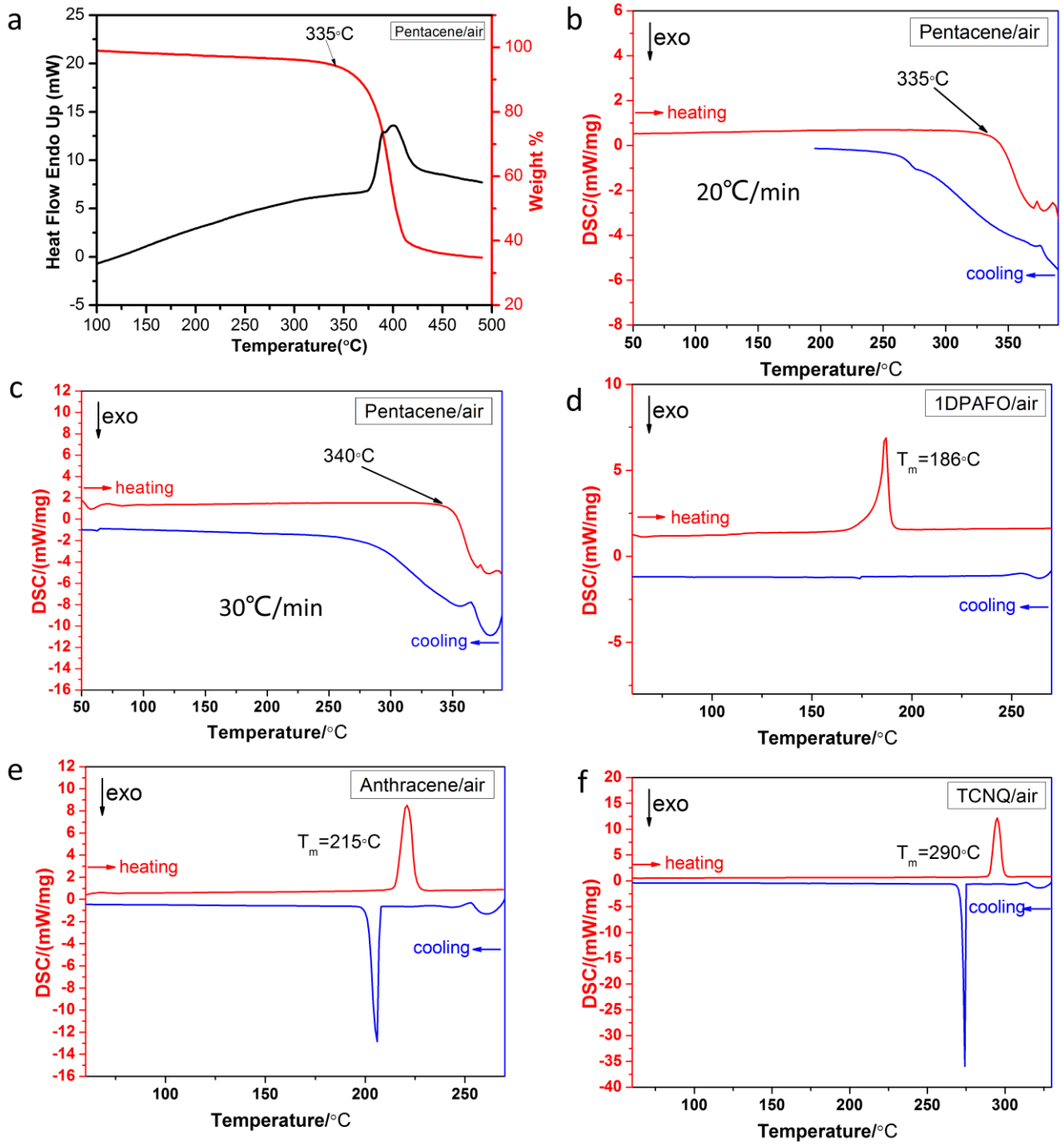

Figure S17 TG/DSC (a) and DSC (b-f) analyses for pentacene (a-c), 1DPAFO (d), anthracene (e) and TCNQ (f) in air at a rate of 10 °C min^{-1} (a, d-f), 20 °C min^{-1} (b) and 30 °C min^{-1} (c).

19. Comparison of PVT and Microspacing In-air Sublimation for growth of organic crystals on substrate

Table S 2 Comparison of PVT and Micro-spacing In-air Sublimation for growth of organic crystals on substrate.

Comparison of PVT and Microspacing In-Air Sublimation for growth of organic crystals on substrate		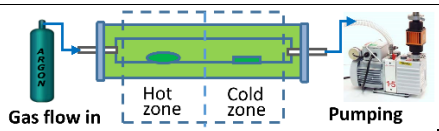 PVT	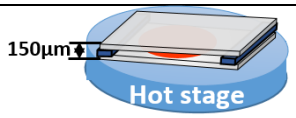 Microspacing In-Air Sublimation Growth
Apparatus and growth parameter	Vacuum system	Required	Not required
	Inert / carrier gas	Required	Not required
	Growth chamber	Required	Not required
	Apparatus size	Large (need supplementary gas cylinder and pump)	Small (only one heater)
	Growth time	Several to tens of hours	5-10 min for organic semiconductor, 1-2 h for pharmaceutical crystal
	Temperature control	Two separate temperature control	One temperature control
Crystal and material	Crystal quality	High	High
	Crystal size	μm - cm	μm
	Dosage for one growth	~ mg	~ 0.01mg
	Material utilization ratio	Low (many crystals grow outside the substrate)	High (nearly all the materials grow into crystals on the substrate)
	Universality to materials	Common organic semiconductors	Common organic semiconductors, stable pharmaceutical compounds
Mechanism	In-situ process observation	Not applicable	Applicable
	Mechanism of crystallization	Vapor-to-crystal	Vapor–to-melt-to-crystal

20. Experiment Section

Fourier transform infrared spectroscop spectra of the samples were accquied on a Nicolet NEXUS 670 Fourier transformation infrared (FTIR) spectrometer. The MALDI-TOF spectras were recorded on a MALDI-TOF instrument (AXIMA Performance, Shimadzu). Elements analysis of by combustion method was carried out using an elemental analyzer (Vario el Z III Z III).